

## Measurement of thermal-energy charge-transfer rate coefficient of $\text{Mo}^{6+}$ and argon

Victor H. S. Kwong, Z. Fang, Y. Jiang, and T. T. Gibbons

*Department of Physics, University of Nevada, Las Vegas, 4505 Maryland Parkway, Las Vegas, Nevada 89154*

L. D. Gardner

*Harvard-Smithsonian Center for Astrophysics, 60 Garden Street, Cambridge, Massachusetts 02138*

(Received 31 January 1992)

The charge-transfer rate coefficient of  $\text{Mo}^{6+}$  and argon has been measured at mean ion energies of 8.8 and 1.4 eV using a laser-ablation ion source and an ion trap. The rate coefficient deduced from these measurements is  $1.02(0.10) \times 10^{-10} \text{ cm}^3 \text{ s}^{-1}$  and appears to be independent of the mean ion energy at this energy range. However, the measured value is an order of magnitude smaller than the Langevin rate coefficient.

PACS number(s): 34.70.+e, 32.80.Pj, 52.50.Jm, 52.25.Vy

### I. INTRODUCTION

The equilibrium processes in man-made and natural plasmas are known to be affected in various ways by the presence of multiply charged ions [1]. Charge transfer between multiply charged ions and neutral species [2] is one way that plasma equilibria can be altered. Extensive theoretical treatments have been carried out in the past two decades to understand these processes and to calculate their cross sections and rate coefficients [3]. A number of experimental programs [4,5] aimed at measurement of electron-capture cross sections and rate coefficients have occurred in parallel with the theoretical efforts.

Some of the results obtained have been used to explain the ionization balance in interstellar media, supernovae remnants, and planetary nebulae [6]. However, especially since the energy crisis in the early 1970s studies have been focused on processes relevant to fusion plasmas [7]. The primary goal has been to understand the radiation loss mechanisms which are closely linked to electron-capture processes in fusion plasmas by highly stripped complex ions of tungsten, molybdenum, titanium, and iron originating from materials making up the limiter and reactor wall [8]. Very little experimental work has been carried out on electron capture of multiply charged ions and neutral species at energies comparable to the edge conditions in fusion plasmas. Most of the experimental work has been carried out at keV collision energies, a regime that is relevant to the study of neutral beam heating [9].

One experimental technique that is suited to measurements in this low energy range uses the ion trap [4,10]. The approach extends the studies to collision energies below those achievable in merged beam experiments [11]. However, all the experimental work involved in these studies has been on multiply charged ions of light elements such as nitrogen, oxygen, carbon, and others where the source for the ions is available as a gas. No experimental work has been reported on low-energy charge transfer of multiply charged ions from refractory ele-

ments present at the edge of the Tokamak fusion plasmas. Recently, Kwong [12] has introduced a novel approach that virtually eliminates the limit on the source of ions by combining a laser-ablation ion source with an ion trap. The technique was demonstrated by measuring the charge-transfer rate coefficient between  $\text{W}^{2+}$  and Ar in the electron-volt energy range [13]. In this paper, we will discuss a measurement for  $\text{Mo}^{6+}$  and Ar. This is the first step toward studies involving multiply charged ions and atomic hydrogen, measurements directly applicable to the conditions present at fusion plasma edges.

### II. EXPERIMENTAL METHOD

The apparatus used in this study has been described earlier [13]. In order to improve the collection efficiency of the ion optics for the detector, the quadrupole mass filter was replaced by a high transmission time-of-flight (TOF) mass spectrometer made from a channel electron multiplier mounted a few centimeters from one of the ion trap's end caps. With this arrangement, the whole ion cloud (with a radius of about a centimeter) was visible to the detector. Systematic effects associated with cooling of the ions by elastic collisions with the target gas, a process that modifies the size of the ion cloud over times comparable to the storage time, were thereby eliminated. However, the short flight path of the spectrometer limited its mass resolution to  $M/dM = 2.5$  at 14 amu, and so the ions were selected by careful choice of the trap's operating parameters, e.g., the frequency  $\Omega/2\pi$  of the rf field at the ring electrode, the amplitude  $V_0$ , and the dc bias  $U_0$  of the rf field. These parameters define the operating point for trapping ions of a specific mass-to-charge ratio and they also determine the well depth and the maximum number of ions stored in the trap. It will be apparent later that the selectivity of the trap is not sufficient to resolve the product ions from a few times ionized Ar formed by electron transfer. Additional measures were introduced to reveal the composition of the stored ions.

Molybdenum ions from laser-ablation plasmas can be

in a variety of charge and internal energy states. Several different charge states can be simultaneously stored in the rf trap for a particular choice of operating parameters. Therefore the parameters must be judiciously chosen to avoid systematic errors. Figure 1(a) shows the operating points for several charge states of molybdenum ions in the stability diagram of a rf trap. The trapping parameters used here have been chosen for maximum density

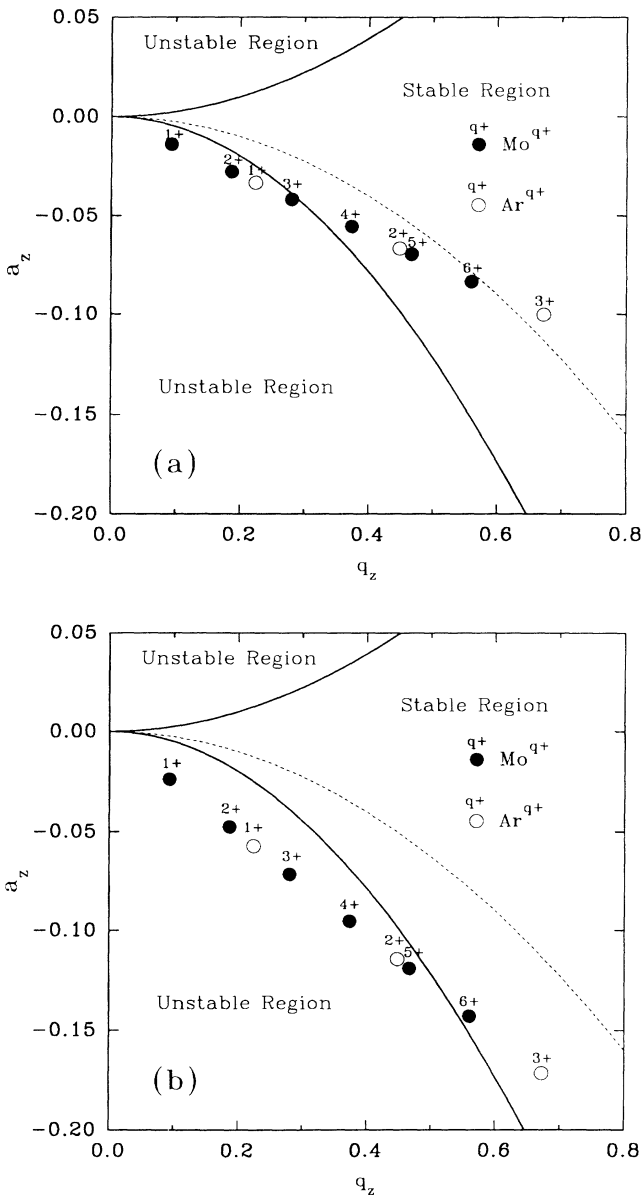


FIG. 1. Stability diagrams for molybdenum and argon ions in a radio frequency ion trap at two different parameter settings. (a) The parameters are set at  $f=0.945$  MHz,  $V_0=345$  V,  $U_0=25.7$  V.  $\text{Mo}^{6+}$  ions are stored in an 88.5-eV ( $qD_r=qD_z$ ) spherical potential well. The potential well for  $\text{Ar}^{2+}$  is nonspherical with 16.7 eV ( $qD_z$ ) along  $z$  direction, the axis of symmetry of the cylindrical trap. (b) The trap parameters are  $f=0.945$  MHz,  $V_0=345$  V,  $U_0=44$  V. Both  $\text{Mo}^{6+}$  and  $\text{Ar}^{3+}$  are stored in the trap. The well depth for  $\text{Mo}^{6+}$  is nonspherical with 14.3 eV ( $qD_z$ ) along the  $z$  direction.

and stability for  $\text{Mo}^{6+}$  [13]. However, other molybdenum ions such as  $\text{Mo}^{4+}$  ( $m/q=24$ ),  $\text{Mo}^{5+}$  ( $m/q=19.2$ ),  $\text{Mo}^{7+}$  ( $m/q=13.7$ ), and  $\text{Mo}^{8+}$  ( $m/q=12$ ) can also be trapped. In particular, the production of  $\text{Mo}^{5+}$  requires 68.45 eV less energy than  $\text{Mo}^{6+}$ . It is therefore reasonable to expect that a significant amount of  $\text{Mo}^{5+}$  will be produced and stored in the trap with  $\text{Mo}^{6+}$ . The limited mass resolution of the TOF mass spectrometer could not distinguish  $\text{Mo}^{6+}$  from  $\text{Mo}^{5+}$ ,  $\text{Mo}^{6+}$  from  $\text{Mo}^{7+}$ , and  $\text{Mo}^{7+}$  from  $\text{Mo}^{8+}$ . The signal from the detector can have contributions from all of the above ions. However, with the combination of proper choice of ablation-laser power density and trapping parameters of the ion trap, molybdenum ions other than  $\text{Mo}^{6+}$  can be excluded from the trap.

The  $\text{Mo}^{6+}$  ion is kryptonlike. The energy required to ionize this kryptonlike ion is 126.5 eV. We therefore can control the production of the higher charge states by limiting the temperature of the ablation plasma by limiting the ablation-laser power density. With laser power density set at or below  $5 \times 10^9$  W cm $^{-2}$ , no charge states beyond  $\text{Mo}^{6+}$  were seen. The power density of the laser was kept well below this value throughout the study.

Charge states lower than  $\text{Mo}^{6+}$  could be excluded from the trap by a proper choice of the trapping parameters. Figure 1(b) shows the operating points for several charge states of  $\text{Mo}^{q+}$  ions with  $q < 6$ , shifted outside the stable region. This was obtained by setting the dc bias at the ring electrode to 44 V. However, at these trapping parameters, the operating point for  $\text{Mo}^{6+}$  was shifted to the edge of the stability region. This reduced the number of stored  $\text{Mo}^{6+}$  by approximately a factor of 10 [13].

We adopt the following scheme to maintain the maximum density for  $\text{Mo}^{6+}$  ions and to eliminate all molybdenum ions with lower charge states. The trap parameters were set for a spherical potential well which allows for maximum  $\text{Mo}^{6+}$  storage [see Fig. 1(a)]. However, immediately after ions were created and trapped, molybdenum ions with charge state lower than 6 were ejected from the trap by rapidly pulsing the trap dc bias,  $U_0$  to 44 V for 5 ms. This dc bias was again applied to the ring electrode for another 5 ms immediately before the stored ions were extracted from the trap for analysis. This second shift on the dc bias ensured that no molybdenum ions with charge states less than 6 formed during the storage phase by charge transfer of  $\text{Mo}^{6+}$  with Ar were visible to the detector. Since this dc bias length is approximately 32 times shorter than the self-equilibrium time of 168 ms [14], the equilibrium energy ( $qD/10=8.85$  eV) of the stored  $\text{Mo}^{6+}$  ions [14,15] was not expected to change appreciably.

The following summarizes the experimental procedure. Ar gas was admitted to the vacuum chamber raising the pressure to a value measured with a calibrated [13] ion gauge.  $\text{Mo}^{6+}$  were created by laser ablation and were cooled and stored in the ion trap. At a delay time  $t$  relative to the ablation event, ions were extracted from the trap by applying to the end cap facing the detector a 1- $\mu$ s extraction pulse of  $-75$  V. After a short time of flight, the extracted ions were detected by a channel electron multiplier. The time-of-flight mass spectrum was record-

ed by a transient digitizer for later analysis. The storage time was scanned from its minimum value by increasing the delay time for a fixed increment  $t$  after each measurement until the ion signal intensity had dropped by one decade from its value at the shortest time delay. The storage time was then scanned in the opposite direction by decreasing the delay time for fixed  $t$  until the shortest delay time (0.5 s) set for the current system was reached. The cycle was then repeated. During each cycle, two data points were obtained for each time delay. Ten such cycles were used to obtain the data for analysis. Each data point in Fig. 2 represents an average of 20 measurements. This procedure was used to minimize any effects due to a possible gradual decrease in the number of stored ions in the trap as a result of the changing conditions on the target surface from laser ablation. The entire procedure was then repeated for a number of different Ar pressures.

The decay of the stored  $\text{Mo}^{6+}$  ions can be described by a simple exponential decay equation:

$$N(t) = N_0 e^{-At}, \quad (1)$$

with

$$A = n(\text{Ar})\langle v_1 q_1 \rangle + n(B_g)\langle v_2 q_2 \rangle + n(\text{Ar})\langle v_1 q_3 \rangle + n(B_g)\langle v_2 q_4 \rangle, \quad (2)$$

where  $n(\text{Ar})$  is the argon gas density,  $n(B_g)$  is the background gas density,  $q_{1,2}$  are the charge-transfer cross sections to all channels including single- and multielectron transfer,  $v$  is the relative velocity of the interacting multiply charged ions and neutral species, and  $q_{3,4}$  are the elastic collision cross sections. Since the  $\text{Mo}^{6+}$  ions were stored in a potential well of depth of 88.5 eV, the probability of  $\text{Mo}^{6+}$  ions being lost from the trap due to elastic collisions with the target gas atoms at room temperature (0.2 eV) was therefore very small. This loss mechanism could be ignored in the analysis.

The slope of the  $\ln[N(t)/N_0]$  versus  $t$  of Eq. (1) gives

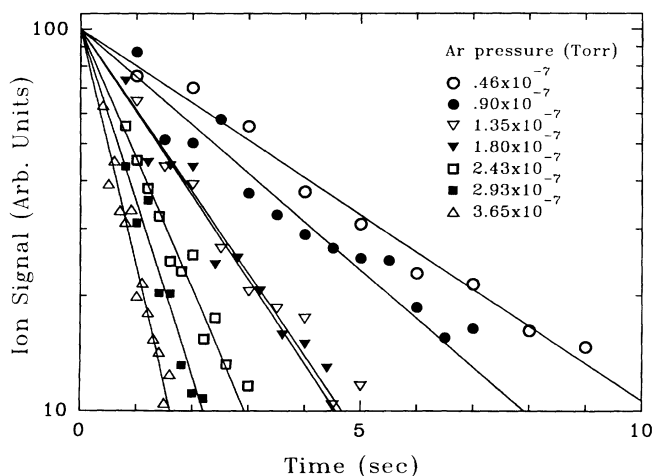


FIG. 2. The decay curves of  $\text{Mo}^{6+}$  ion signal vs time in different Ar pressures.

the value of charge-transfer rate,  $A$ , for a given Ar gas density. The slope of  $A$  versus Ar density in Eq. (2) gives the charge-transfer rate coefficient  $\langle v_1 q_1 \rangle$  between  $\text{Mo}^{6+}$  and Ar. The intercept gives the charge-transfer rate  $n(B_g)\langle v_2 q_2 \rangle$  of  $\text{Mo}^{6+}$  ions and residual background gas atoms present in the ultrahigh-vacuum system. The background gas is composed mainly of water and hydrogen, as determined using a residual gas analyzer.

### III. EXPERIMENTAL RESULTS AND DISCUSSION

Figure 2 is a plot of ion signal intensities versus delay time for seven Ar gas pressures. Figure 3(a) is a plot of the  $\text{Mo}^{6+}$  signal decay rate versus pressures. The slopes in the figures are obtained by weighted least-squares fits to exponential and linear functions, respectively. The scatter on the data points is due to the fluctuations of the ion signals. The rate coefficient for  $\text{Mo}^{6+}$  and Ar obtained from the slope of Fig. 3(a) is  $1.02(0.10) \times 10^{-10}$

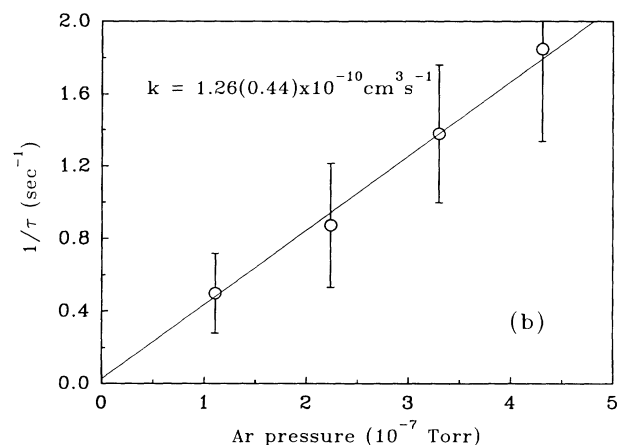
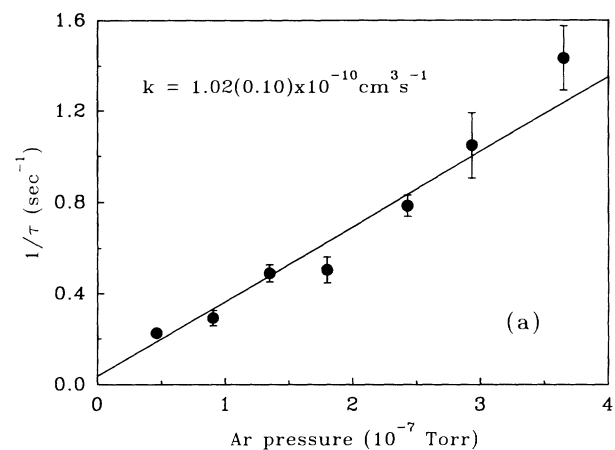


FIG. 3.  $\text{Mo}^{6+}$  decay rate vs Ar pressure. The slope of the straight line fit gives the charge-transfer rate coefficient. (a) Potential well depth is 88.5 eV ( $qD_x = qD_z$ ). (b) Potential well depth is 14.3 eV ( $qD_z$ ).

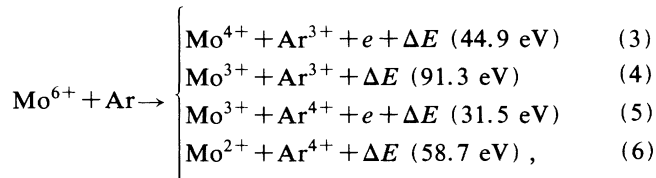
$\text{cm}^3 \text{s}^{-1}$ . The charge-transfer rate of  $\text{Mo}^{6+}$  and the residual background gas in the vacuum chamber obtained from the intercept at zero pressure is  $0.03(0.05) \text{ s}^{-1}$ . The uncertainties presented are computed from the uncertainties of the Ar density measurements and the fluctuation of the ion signal intensities as indicated from the fits.

The charge-transfer rate of  $\text{Mo}^{6+}$  and the residual gas was confirmed by observing the decay of  $\text{Mo}^{6+}$  at the base pressure of the ultrahigh-vacuum system. The ion loss rate is determined to be  $0.025(0.002) \text{ s}^{-1}$ . This rate is consistent with that obtained at the intercept of Fig. 3(a).

The equilibrium energy of the stored ion in rf trap is known to be approximately a tenth of the potential well depth  $qD$  [14,15]. This fact was used to provide information regarding the energy dependence of the rate coefficient. The measurement was repeated with the dc bias  $U_0$  at 44 V and other trap parameters unchanged. The axial potential well depth for  $\text{Mo}^{6+}$  was reduced from 88.5 to 14.3 eV ( $=qD_z$ ), thereby altering the equilibrium ion energy from 8.85 to 1.43 eV. Furthermore, as a side benefit, molybdenum ions with charge state lower than 6 were excluded from the trap [see Fig. 1(b)]. Figure 3(b) is a plot of the  $\text{Mo}^{6+}$  decay rate as a function of Ar pressure. The rate coefficient is  $1.25(0.44) \times 10^{-10} \text{ cm}^3 \text{ s}^{-1}$ . The larger uncertainty in this measurement is primarily due to a much smaller signal-to-noise ratio. This rate coefficient obtained at a shallower well depth is the same, within experimental uncertainty, as the value we obtained at the greater well depth. The invariance on the rate coefficient at two ion equilibrium energies suggests that the cross section is inversely proportional to the velocity in accordance with the orbiting model [16] for electron capture. The measured rate coefficient is an order of magnitude smaller than the Langevin rate coefficient,  $1.69 \times 10^{-9} \text{ cm}^3 \text{ s}^{-1}$ . The discrepancy between the measured rate and the Langevin rate may be explained by the fact that the Langevin model is based on ion-molecule interaction where charge transfer can take place through many of the rotational and vibrational channels of the molecule. In an atom-ion reaction, however, there are only a few selected channels leading to charge transfer. These are probably the high  $n$  states, with the transfer occurring at large distances where the probability is likely small.

As was discussed earlier, the ions with mass-to-charge ratio greater than 18 amu can be excluded from the trap by shifting the dc bias on the ring electrode  $U_0$  to 44 V prior to the extraction of ions from the trap for analysis. This, however, cannot exclude the product ions with mass  $16 < m$  and  $q < 8$ . Ions such as  $\text{Ar}^{3+}$  (13.33 amu) and  $\text{Ar}^{4+}$  (10 amu) formed as the result of multielectron transfer cannot be excluded from the trap if their energies are less than that of the trapping potentials.

The ionization energy required to produce  $\text{Mo}^{6+}$  from its neutral ground state is about 226 eV. Multiple electron capture is exothermic and will likely occur [17]. Some of the electron transfer channels which result in the formation of  $\text{Ar}^{4+}$  and  $\text{Ar}^{3+}$  are outlined in the following:



where  $\Delta E$  is the maximum kinetic energy shared by the ion pairs in their ground states. It was estimated based on the differences of ionization energies. Since these product ions are not normally formed in their ground states, the actual kinetic energies available to them may be less. However, this gives the upper bound of the kinetic energy available to the ion pairs. Other reactions such as those which include subsequent electron capture by the product ions and Ar target gas are not considered here.

We have estimated the kinetic energies of the product  $\text{Ar}^{3+}$  and  $\text{Ar}^{4+}$  ions in the multielectron transfer processes listed in Eqs. (3)–(6). For the channel [Eqs. (3) and (5)] involving autoionization with the formation of  $\text{Ar}^{3+}$  and  $\text{Ar}^{4+}$  and an autoionized electron, the kinetic energy of the product  $\text{Ar}^{3+}$  and  $\text{Ar}^{4+}$  is 31.8 and 22.24 eV, respectively. The kinetic energy of the product  $\text{Ar}^{4+}$  ion for the four-electron capture [Eq. (6)] is found to have a maximum value of 41.36 eV while the product  $\text{Ar}^{3+}$  ion for three-electron transfer [Eq. (4)] is 64 eV. The potential wells created by the ion trap for  $\text{Ar}^{3+}$  and  $\text{Ar}^{4+}$  at the parameters chosen to optimize for  $\text{Mo}^{6+}$  are estimated to be 53.4 and 83.6 eV, respectively. Since their kinetic energies are less than the trapping potential,  $\text{Ar}^{3+}$  and  $\text{Ar}^{4+}$  so formed could have been stored in the trap. The selectivity of the trap was not adequate to resolve this. Additional detector resolution was therefore required to evaluate the systematic effect.

A 1-m time-of-flight mass spectrometer with mass resolution of  $M/dM = 11.4$  at 16 amu was built and installed in the ion trap facility to examine in more detail the content of the trap qualitatively. However, this spectrometer can only sample a fraction of the trap's content due to a small solid angle subtended on the ion cloud by the detector. During this test, the ion trap was set as before to provide a spherical well for  $\text{Mo}^{6+}$ , and no attempt was made to shift the dc bias to exclude both  $\text{Mo}^{5+}$  and  $\text{Mo}^{4+}$  ions. Figure 4 is a typical TOF mass spectrum of the ions extracted from the ion trap at a storage time of 3 s. Clearly neither  $\text{Ar}^{3+}$  nor  $\text{Ar}^{4+}$  was observed in the mass spectrum, indicating that these ions were absent from the trap. Their absence may not be surprising, since the charge-transfer rates of Ar ions and atoms are an order of magnitude larger than the rate for  $\text{Mo}^{6+}$  and Ar that we measured here [17,18]. Any  $\text{Ar}^{3+}$  and  $\text{Ar}^{4+}$  ions formed by multielectron transfer could be removed from the trap by rapid charge transfer to  $\text{Ar}^{2+}$  which could then leave the trap because of their high kinetic energy inherited from their parents,  $\text{Ar}^{3+}$  and/or  $\text{Ar}^{4+}$ , and the kinetic energy acquired during their formation. The potential well for  $\text{Ar}^{2+}$  is estimated to be 16.8 eV and is too shallow to confine them.

It was also interesting to find that only very small quantities of  $\text{Mo}^{5+}$  were found in the TOF mass spec-

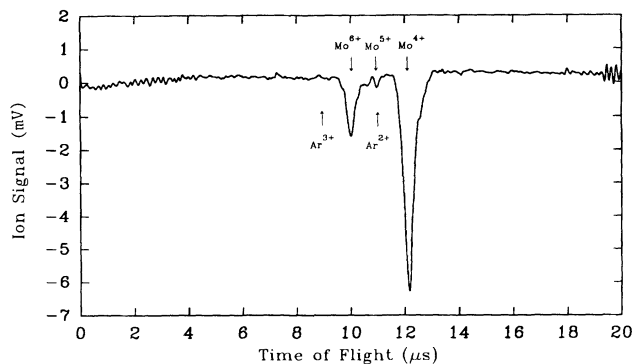


FIG. 4. Typical time-of-flight mass spectrum of stored ions at parameter setting corresponds to Fig. 1(a). Two intense peaks corresponding to  $\text{Mo}^{6+}$  and  $\text{Mo}^{4+}$  are present. A small peak that corresponds to  $\text{Mo}^{5+}$  and/or  $\text{Ar}^{2+}$  is present. No  $\text{Ar}^{4+,3+}$  are detected. The TOF spectrometer has been previously calibrated using  $\text{Ar}^+$ ,  $\text{Ar}^{2+}$ ,  $\text{N}_2^+$ ,  $\text{N}^+$ .

trum. We attribute this to a much higher electron-capture rate with the formation of lower charge state product ions such as  $\text{Mo}^{4+}$ . One can draw some conclusions about the relative size of the rate coefficients for  $\text{Mo}^{5+}$  and  $\text{Mo}^{4+}$ . The absence of  $\text{Mo}^{5+}$  and the presence

of  $\text{Mo}^{4+}$  suggests that the rate coefficient for  $\text{Mo}^{5+}$  is substantially higher than the rate for both  $\text{Mo}^{6+}$  and  $\text{Mo}^{4+}$  and that the rate for  $\text{Mo}^{4+}$  is comparable to  $\text{Mo}^{6+}$ . Work on  $\text{Mo}^{5+}$  and  $\text{Mo}^{4+}$  is currently in progress.

#### IV. CONCLUSION

We have measured the charge-transfer rate coefficient for  $\text{Mo}^{6+}$  and Ar at equilibrium energies of 8.8 and 1.4 eV. The rate coefficient is  $1.02(0.10) \times 10^{-10} \text{ cm}^3 \text{ s}^{-1}$  and appears to be independent of the ions' mean energies, which suggests that the cross section is inversely proportional to the relative velocity. However, our measured value is an order of magnitude smaller than the Langevin rate coefficient.

#### ACKNOWLEDGMENTS

We acknowledge the technical assistance of Heinze Knocke and Milton Lewis. Critical comments from W. H. Parkinson and S. Bliman are also appreciated. This work is supported in part by Grant No. RII-8410674 from the National Science Foundation (EPSCoR) to the University of Nevada system. One of the authors (V.H.S.K.) thanks the Smithsonian Institution for financial support which has allowed this paper to be completed at the Harvard-Smithsonian Center for Astrophysics.

- [1] A. Dalgarno, in *Physics of Ion-Ion and Electron-Ion Collisions*, edited by F. Brouillard and J. W. McGowan (Plenum, New York, 1983), pp. 1–36; D. E. Post, *ibid.*, pp. 36–99.
- [2] D. A. Neufeld and A. Dalgarno, *Phys. Rev. A* **35**, 3142 (1987); H. Tawara and W. Fritsch, *Phys. Scr.* T28, 58 (1989).
- [3] R. K. Janev and L. P. Presnyakov, *Phys. Rep.* **70**, 1 (1981); R. McCarroll and P. Valiron, *Astron. Astrophys.* **53**, 83 (1976).
- [4] D. A. Church and H. M. Holzschleiter, *Phys. Rev. Lett.* **49**, 643, (1982).
- [5] R. A. Phaneuf, I. Alvarez, F. W. Meyer, and D. A. Crandall, *Phys. Rev. A* **26**, 1892 (1982).
- [6] D. Flower, *Molecular Collisions in the Interstellar Medium* (Cambridge University Press, Cambridge, England, 1990), p. 91.
- [7] H. Tawara and W. Fritsch, *Phys. Scr.* T28, 58 (1989).
- [8] R. V. Jensen and D. E. Post, *Nucl. Fusion* **17**, 1187 (1977).
- [9] H. B. Gilbody, in *Advances in Atomic and Molecular Physics*, edited by D. Bates (Academic, New York, 1986), Vol. 22, 143.
- [10] C. R. Vane, M. H. Prior, and Richard Marrus, *Phys. Rev. Lett.* **46**, 107 (1981).
- [11] C. C. Havener, M. S. Hug, H. F. Krause, P. A. Schulz, and R. A. Phaneuf, *Phys. Rev. A* **39**, 1725 (1989).
- [12] V. H. S. Kwong, *Phys. Rev. A* **39**, 4451 (1989).
- [13] V. H. S. Kwong *et al.*, *Rev. Sci. Instrum.* **61**, 1931 (1990).
- [14] R. A. Heppner, F. L. Walls, W. T. Armstrong, and G. H. Dunn, *Phys. Rev. A* **13**, 1000 (1976).
- [15] D. A. Church and H. G. Dehmelt, *J. Appl. Phys.* **40**, 3421 (1969).
- [16] D. Flower, *Molecular Collisions in the Interstellar Medium* (Cambridge University Press, Cambridge, England, 1990), p. 84.
- [17] L. Liljeby *et al.*, *Phys. Scr.* **33**, 310, (1986).
- [18] K. Okuno and Y. Kaneko, *Shitsuryo Bunseki, Mass Spectroscopy* **34**, 351 (1986).